Bulletin of Electrical Engineering and Informatics
Vol. 14, No. 4, August 2025, pp. 2649~2661
ISSN: 2302-9285, DOI: 10.11591/eei.v14i4.8010

Analysis of unmanned aerial vehicle airframe materials on circularly polarized antenna radiation characteristics

Wahyudi[1], Imas Tri Setyadewi[1], Mohammad Amanta Kumala Sakti[1], Yanuar Prabowo[1] , Donatina Miswati Hadiyanti[1], Novelita Rahayu[1], Nurul Lailatul Muzayadah[1], Agus Hendra Wahyudi[1,2], Yomi Guno[1,3], Teguh Praludi[4], Cahya Edi Santosa[1], Josaphat Tetuko Sri Sumantyo[5,6]
[1]Research Center for Aeronautics Technology, National Research and Innovation Agency (BRIN), Bogor, Indonesia
[2]Department of Electrical Engineering, Faculty of Engineering, Pamulang University, Banten, Indonesia
[3]School of Electrical Engineering and Informatics, Bandung Institute of Technology, Bandung, Indonesia
[4]Research Center for Telecommunication, National Research and Innovation Agency (BRIN), Bandung, Indonesia
[5]Center for Environmental Remote Sensing (CEReS), Chiba University, Chiba, Japan
[6]Department of Electrical Engineering, Faculty of Engineering, Sebelas Maret University, Solo, Indonesia

Article Info

Article history:

Received Dec 11, 2023
Revised Mar 10, 2025
Accepted May 27, 2025

Keywords:

Airborne synthetic aperture radar
Circular-polarization
Material composites
Microstrip antenna
Unmanned aerial vehicle

ABSTRACT

This paper presents an experimental examination of how unmanned aerial vehicle (UAV) airframe materials affect the electromagnetic characteristics of the airborne circularly polarized (CP) payload antenna. This study specifically investigates the received signal from the circularly polarized synthetic aperture radar (CP-SAR) antenna installed within the fuselage of the lapan surveillance UAV (LSU). In the airborne CP-SAR experiment, broadband CP microstrip subarray antennas were used along with LSU series airframe material composites comprising E-glass EW-185 and Carbon C522 Twill. The composite specimens were prepared to have the same size and thickness to minimize variability in the comparative analysis. The experimental study measures the transmission loss using S-parameters. At 5.3 GHz, the E-glass EW-185 fiber composite exhibits a material attenuation of -1.5 dB and a circular depolarization of 0.32 dB. The E-glass EW-185 fiber composite exhibits a material attenuation of -1.5 dB and a circular depolarization of 0.32 dB. In contrast, the Carbon C522 Twill fiber composite demonstrates a significantly higher material attenuation of -31.24 dB and a circular depolarization of 10.70 dB. Additionally, this paper examines the radiation pattern measurements of the CP-SAR antenna at various frequencies, providing a comprehensive analysis of the materials' impact on antenna performance.

Corresponding Author:

Wahyudi
Research Center for Aeronautics Technology, National Research and Innovation Agency (BRIN)
Bogor, Indonesia
Email: wahy023@brin.go.id

1. INTRODUCTION

In the era of advancing technology, the use of unmanned aerial vehicles (UAVs) for various applications has become prominent, including mapping, surveillance, and monitoring, all of which rely heavily on the capabilities of the payload mounted on the UAV [1]. Regarding remote sensing applications, synthetic aperture radar (SAR), as a UAV-based active imaging radar, has an active imaging radar that generates a signal to illuminate the target. This capability allows SAR systems to operate in almost all-weather conditions, including cloudy, foggy, or nighttime scenarios. Compared to conventional airborne or space-borne SAR systems [2]–[5], UAV SARs also have other advantages, including low cost, low risk,

high-resolution imagery, improved accuracy, faster data processing, operational efficiency, compact size, and real-time functionality. Traditional SAR systems primarily use linearly-polarized (LP) microwave supported by high-power RF amplifiers in various polarimetric modes (VV, HH, VH, and HV) [6]–[9]. Unfortunately, LP microwaves on a SAR system implementation onboard satellite are sensitive to Faraday rotation phenomena. This phenomenon slightly alters the LP microwave's orientation angle as it propagates through the ionosphere layer, resulting in polarization mismatch and reduced received power of the scattering signal from the target. Therefore, the orientation angle of the received signal must be corrected during SAR data processing [10], [11]. The polarization mismatch issues in LP microwaves can be mitigated by using circularly polarized (CP) microwaves [12].

One of the biggest challenges in producing UAVs for SAR applications is managing the material structure's weight, as it directly affects UAV performance. Generally, to reduce weight while maintaining structural strength, UAVs are made from composite materials as they have high flexibility, strength, and lightness compared to metal materials. Indonesia's National Research and Innovation Agency (BRIN) has developed UAVs weighing between 10 kg and 80 kg, with various fuselage composite materials such as fiberglass, carbon, and Kevlar, [13], [14]. Other research has been conducted on the mechanical properties of composite materials, including comparative studies between E-glass, carbon fiber, and hybrid (carbon & E-glass). The findings of these studies indicate that while E-glass excels in high strength and ease of fabrication, with a composite tensile strength of 354.992 MPa and an compression strength of 31.080 Mpa using UTM test, carbon fiber offers significantly higher structural strength and lighter weight, exhibiting a composite tensile strength of 217.445 MPa and an compression strength of 12.312 Mpa, hybrid (carbon & E-glass) exhibiting a composite tensile strength of 314.554 MPa and an compression strength of 21.211 Mpa using UTM test. These results indicate that carbon fiber outperforms E-glass and hybrid terms of strength and lightness [15].

Another issue in designing airborne SAR systems is the signal loss caused by microwave propagation through the material structure of an airborne pod or fuselage. The type, composition, and thickness of materials used in the pod, radome, or fuselage present a trade-off between their physical strength and the electrical properties that affect SAR signal propagation. The effect of materials on electromagnetic characteristics has been investigated in [16], and issues related to circular polarization wave depolarization in different media have been discussed in [10], [17]. Another research [18] shows that using carbon fiber and polymaterial materials in the radome installed on the Cesna 172 aircraft to protect the SAR antenna can cause signal attenuation ranging from 1 dB to 30 dB, significantly impacting the quality of the received signal. Hence, the installation of the SAR antenna must meet specific electrical property criteria, including gain and 3-dB beamwidth. Table 1 shows the target specifications for airborne SAR antenna installations.

Table 1. Target specifications of the CP-SAR system design onboard airborne [13]

Symbols	Parameter	Value
f_c	Center frequency	5.3 GHz
B	Operating bandwidth	400 MHz
G	Antenna gain	>20 dBic
P	RF power amplifiers	200 Watt
θ_{ra}	Range beam-width	10^0 (E-plane)
ϕ_{az}	Azimuth beam-width	5^0 (H-plane)
AR	Polarization (Tx/Rx)	<3 dB (RHCP+LHCP)
h	Flight altitude	1000 meters

The Center for Environmental Remote Sensing (CEReS), Chiba University Japan, has developed CP-SAR systems onboard airborne and satellite platforms for environmental remote sensing observation. The target specifications of the CP-SAR system onboard airborne are listed in Table 1 [18]. The design of the CP-SAR antenna incorporates a microstrip antenna array installed inside the UAV fuselage. Constraints such as limited space, weight restrictions, gain requirements, and fuselage material attenuation present significant challenges in designing the antenna layout and selecting suitable materials [19]. As part of this investigation, the prototype of the 4×4 broadband CP microstrip antenna is the subarray element of the airborne C-band CP-SAR sensor. The subarray acts as the electromagnetic source for UAV material characteristic testing. The study involves two types of UAV materials: WR 185-type glass fiber and UD carbon fiber. This paper explores how the material composition of the UAV airframe affects the electromagnetic characteristics of the airborne CP-SAR antenna and is structured into five sections: section 2 briefly describes the properties of the CP-SAR subarray antenna; section 3 explains the LSU UAV and its airframe material; section 4 discusses the experimental method and measurement results; and section 5 concludes the findings.

2. PROCEDURE SPECIFICALLY DESIGNED

2.1. The airborne cp-sar subarray antenna

The experimental investigation of the airborne CP-SAR antenna utilizes the prototype of a 4×4 broadband CP microstrip subarray antenna operating in the right-handed circularly polarized (RHCP) mode. A photograph of the prototype antenna is shown in Figure 1.

The detailed design and measured performance of this prototype antenna are discussed in [19]. The antenna prototype is constructed using sandwiched-stacked double substrates which have 1.6 mm thickness (h), 2.17 dielectric constant (єr), 0.0005 dissipation factor (tan-δ), and physical dimension on 10×20×15 cm as shown in Figure 1(a). The antenna design employs a thick substrate with a low dielectric constant to achieve a broader 10-dB impedance bandwidth (IBW). The circular polarization wave generator utilizes the square patch radiator with a diagonal curve corner-truncation, the single-feed proximity-coupled microstrip line feeding. The radiator is placed between two substrates with the construction as shown in Figure 1(b). The circle-slotted parasitic patch above the radiating patch is an additional design to improve the axial-ratio bandwidth (ARBW) and antenna gain. To suppress an undesired electromagnetic field emitted by the complex feeding network in the array configuration, the copper layer covers the top layer of the substrate.

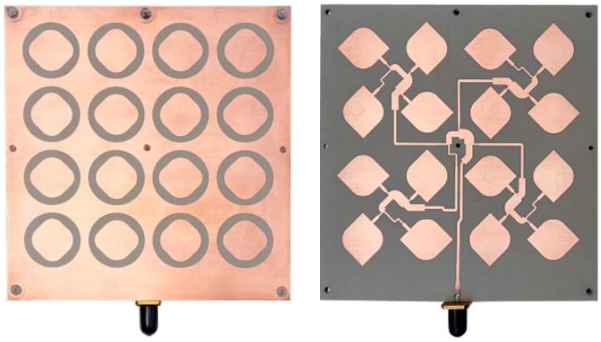

(a) (b)

Figure 1. The prototype of 4×4 broadband CP microstrip subarray antenna; (a) top view and (b) the feeding network configuration

The subarray antenna implements a serial sequential rotation configuration with a uniform patch separation of 0.5 λ. The characteristics of the CP-SAR antenna, such as S-parameter (S_{11}), axial-ratio (AR), gain, and voltage standing-wave ratio (VSWR), are shown in Figure 2.

The shadowed bar in the graph indicates the bandwidth or the operating frequency of the CP-SAR antenna. The measured IBW is S_{11} parameter values below -10 dB as shown in Figure 2(a) approximately 910 MHz (17.17%) along 4.80 GHz to 5.71 GHz. The ARBW is approximately 1180 MHz (22.17%), spreading from 4.83 GHz to 6.01 GHz. Figure 2(b) plots the minimum gain of 13.2 dBic at the frequency of 5.22 GHz and the maximum gain of 16.96 dBic at the frequency of 5.42 GHz. Further, the average gain is 15.0 dBic at the center frequency of 5.3 GHz. The performance of the antenna prototype at the center frequency of 5.3 GHz is summarized in Table 2.

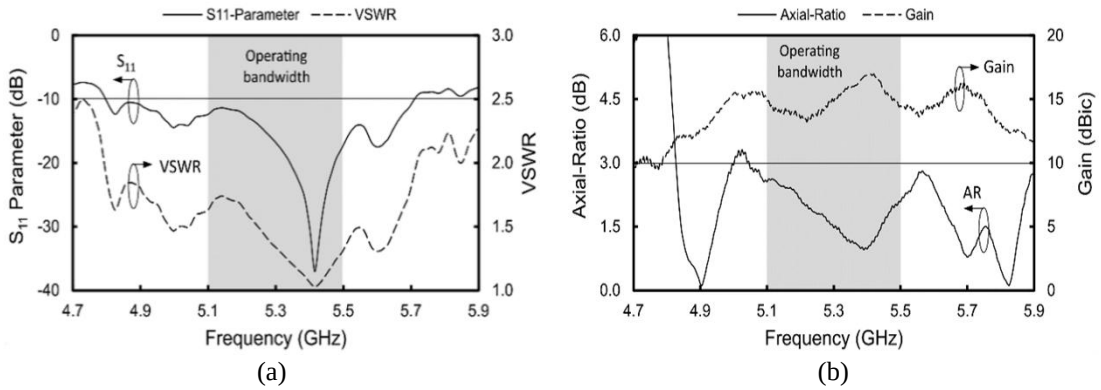

(a) (b)

Figure 2. Electrical characteristics of the CP-SAR antenna; (a) S-parameter (S_{11}) and VSWR and (b) AR and gain

Table 2. Summary of the CP-SAR antenna characteristics configured in the uniform separation of $d_x=d_y=0.5\ \lambda 0$

Parameters		Value	Unit
Return-loss (S_{11})	f_L 4.80 GHz	4.80	GHz
	f_H 5.71 GHz	5.71	GHz
	IBW	910 (17.17)	MHz (%)
AR	f_L	4.83	GHz
	f_H	6.01	GHz
	ARBW	1180 (22.17)	MHz (%)
H-plane (ϕ_{az})	Direction	4.0	degree
	BM	22.0	degree
	SLL	−8.0	dB
E-plane (θ_{rg})	Direction	0.0	degree
	BM	23.0	degree
	SLL	−12.0	dB
Gain		15.0	dBic
Polarization		RHCP	
VSWR (1:2)		1.3	
Dimension ($x\times y$)		132.0×132.0	mm

(Note: BM=beam width, SLL=side-lobe-level, and f_L/f_H=lowest/highest frequency at the bandwidth)

2.2. Lapan surveillance unmanned aerial vehicle

The center for aeronautics technology, part of the National Institute of Aeronautics and Space of Indonesia (LAPAN), has been actively developing fixed-wing UAVs since 2012. In 2021, Lapan and various other research institutions across Indonesia merged and consolidated to form the BRIN. BRIN has developed several fixed-wing UAVs for surveillance and environmental remote sensing applications such as disaster monitoring, agriculture mapping, and crater observation [20], [21]. Until now, BRIN has been successfully flying four variants of the LSU series, each developed in different sizes and capabilities and equipped with specialized sensors, namely LSU-01, LSU-02, LSU-03, and LSU-05. Photographs with detailed specifications of two types of LSU-03 series are shown in Figures 3(a) and (b) respectively.

(a) (b)

Figure 3. The LSU-03 series; (a) fiberglass composite and (b) fiber carbon composite

The LSU-03 series is dedicated to airborne remote sensing applications. The LSU airframe manufacturing uses composite materials, including the main wing, rear wing, fuselage, and landing gear components. There are two types of LSU-03 series based on the substance of the airframe composite material, specifically the LSU-03 and LSU-03 NG series. The LSU-03 (see Figure 3(a)) utilizes plain-weave type woven glass fabric EW-185 composite material and the LSU-03 NG series (see Figure 3(b)) incorporates a carbon C522 twill cloth composite material. The fuselage of the LSU-03 NG employs carbon C522 material due to its mechanical properties, i.e., particularly its lightweight and high strength, which provide significant advantages for both aircraft and watercraft platforms [22], [23].

Generally, both of the LSU-03 series have a structure with the exact specification: a 3.5 meter wingspan, 2.5 meters body length, approximately 10 kg payload weight, equipped with a 100 cc 2-stroke gasoline engine (single propeller), and the ability to fly in a maximum speed of 150 km/h. These specifications were obtained from the National Institute of Aeronautics and Space (Lembaga Penerbangan dan Antariksa Nasional, LAPAN).

3. METHOD

3.1. Structure of composite materials

The LSU airframe components are manufactured by combining layers of epoxy resin and fiberglass or fiber carbon element [15], [24]. The manufacturing process applies the hand lay-up technique by considering its advantages; i.e., ease of processing, a minimum requirement of infrastructure and equipment,

and efficiency on production for a research and development component. In the hand lay-up process, the composite is manufactured using a rubber plate and manually pressed by hand to remove trapped air inside the stacked layers of fiber and matrix. In this research, the specimen of the LSU-03 airframe was made from a composite box with dimensions of 240×140×100 mm. This box will cover the CP-SAR antenna while the measurements are conducted in the anechoic chamber. Two types of specimen composite boxes of the LSU airframes, their structure layers, and surface contour captured by scanning electron microscopy (SEM) tool are depicted in Figure 4.

Figure 4(a) shows the specimen of the composite material consisting of 4 layers of plain-weave type woven glass fabric EW-185 cloth with 0.03 mm thickness and five layers of epoxy resin (Lycal) with 0.22 mm thickness. Both materials are stacked with alternating layers. The manufacturing product of this composite structure has a total thickness of approximately 1.2 mm indicated by a white surface color. From the SEM analysis with 30 times magnification, random surface contours reveal the presence of numerous small holes. Figure 4(b) illustrates a composite specimen combining two layers of Carbon C522 Twill cloth and three layers of epoxy resin (Lycal). Both materials have the same thickness of 0.22 m. The stacked structure of composite CFRP has a total thickness of approximately 1.1 mm, indicated by a woven texture and a black surface color. SEM analysis with 30 times magnification at random locations shows that the surface contour is nearly perfect, though small holes remain. These holes are scarce and smaller in size compared to the EW-185 specimen.

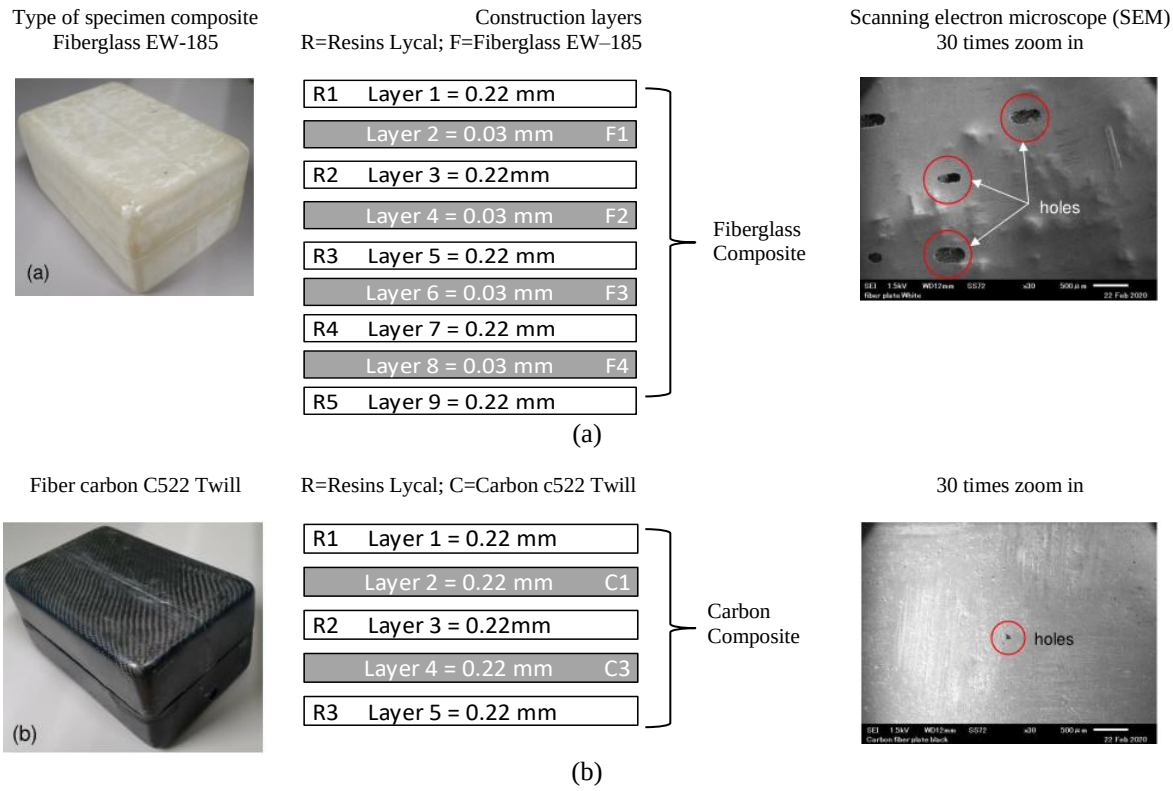

Figure 4. Two types of specimen composites of the LSU airframes with their construction layers and SEM investigations; (a) plain-weave type woven glass fabric EW-185 cloth [14] and (b) mixing carbon C522 twill cloth [15]

3.2. Electromagnetic measurement

Figure 5 illustrates the experimental setup for investigating the electromagnetic characteristics of the CP-SAR signal propagation in the anechoic chamber at Chiba University, Japan. The measurement system consisted of an E8364C PNA microwave network analyzer integrated with a computerized turntable device. The transmitter antenna (Tx) used the 3102 conical log spiral antenna with a gain of approximately 2.5 dBi connected to port 1 of the PNA [25]. The receiver antenna (Rx) used the 4×4 broadband CP microstrip subarray antenna as the CP-SAR sensor, connected to port 2 of the PNA. The two antennas were positioned at a distance of 3.0 meters to satisfy the Fraunhofer distance formula and ensure a plane wave in the far-field region [26], [27].

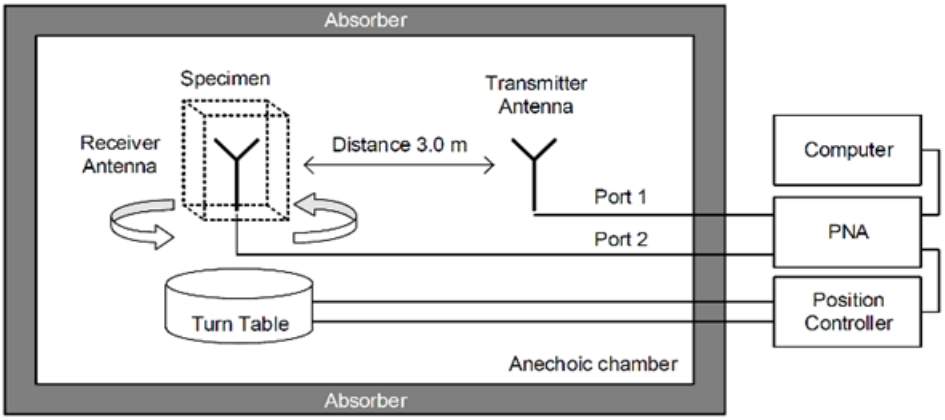

Figure 5. Geometry installation of the measurement system to characterize the attenuation of the CP-SAR antenna onboard the LSU-03 in the anechoic chamber

The methodology of the experimental investigation consists of 3 steps. First, the receiver antenna Rx was installed on the turntable without being covered by the specimen composite box. This measurement aims to collect the reference data of the behavior received power with a free space environment or no obstacle along the line-of-sight (LOS) between Tx and Rx antennas. Second, the Rx antenna was placed inside the specimen composite box of fiberglass EW-185 and installed on the turntable, as shown in Figure 6(a), then, the received power characteristics of the CP-SAR antenna were measured. Further, the third step repeats the second step, with changes in the specimen composite box to fiber carbon C522 Twill box, as shown in Figure 6(b). Both specimen composite boxes are designed to simulate the fuselage of the LSU series.

(a) (b)

Figure 6. Configuration of the 4×4 broadband CP microstrip array antenna as the CP-SAR antenna inside the composite specimen box; (a) fiberglass EW-185 and (b) fiber carbon C522 twill

In 2-port S-parameters concept, the insertion-loss (S_{21}) or received power can theoretically be expressed using Friis's transmission as (1) and (2):

$$\boldsymbol{S_{21}}^{\boldsymbol{2}} = \left[\frac{P_r}{P_t}\right] \tag{1}$$

$$\boldsymbol{S_{21}}^{\boldsymbol{dB}} = {P_L}^{dB} + {G_t}^{dB} + {G_r}^{dB} \tag{2}$$

Where ${P_L}^{dB}$, ${G_t}^{dB}$, and ${G_r}^{dB}$ represent the path-loss in free-space, the gain of transmitter antenna Tx, and gain of receiver antenna Rx, respectively [17]. The the path-loss in free-space can be written as (3) and (4):

$$\boldsymbol{P_L}^{\boldsymbol{dB}} = 20.log_{10}\left[\frac{\lambda}{4\pi d}\right] \tag{3}$$

$$\boldsymbol{P_L}^{\boldsymbol{dB}} = -21.98^{dB} + 20.log_{10}\left[\frac{\lambda}{d}\right] \tag{4}$$

Where λ is a wavelength in free space, and d is the distance between the transmitter antenna Tx and the receiver antennas Rx. By applying (1) to (4), the insertion-loss (S_{21}) at the spreading frequency can be estimated and verified by measuring the received power in port 2. The approximation value of S_{21} at the center frequency of 5.3 GHz is 38.97 dB (λ=0.056 m, d=3.0 m, G_t=2.5 dBi, and G_r=15 dBi).

The quantifying of circular polarization wave is detailed in [10] and is commonly expressed using the AR magnitude as (5) and (6):

$$\boldsymbol{AR^{dB}} = 20.log_{10}|R| \quad (5)$$

$$= 20.log_{10}\left|\frac{1+e}{1-e}\right| \quad (6)$$

where, $e=10^{-PdB/20}$. A perfect circular polarization corresponds to AR=0 dB, while linear polarization field have AR≥ 40 dB until infinity. The P^{dB} value, representing the power of the cross-polarization, is expressed as (7):

$$P^{dB} = \left|{P_{RHCP}}^{dB} - {P_{LHCP}}^{dB}\right| = 10.log_{10}\left|\frac{E^2}{377}\right| \quad (7)$$

where E is the electric field and 377 Ω is the wave impedance in free space.

The quality of the circular depolarization wave is analyzed by comparing the AR of the received signal between the receiver antenna Rx placed in the free space and inside the composite specimen. Circular depolarization deferences are indicated by AR value changes in dB.

4. MEASUREMENT RESULTS

In this work, the material attenuation and circular depolarization caused by the fuselage material of the LSU were investigated by comparing the values of the receiving power on port 2 under two conditions: without any obstacle along the path versus with an obstacle along the path (or when the Rx antenna is installed inside the composite specimens). The fuselage material attenuation was indicated by a reduction in the receiving power (in dB) measured at the Rx antenna (port 2). The measurements of the CP-SAR antenna's material attenuation and circular depolarization are plotted in Figure 7.

A shaded bar in the graph's background marks the operating frequency range of the CP-SAR antenna. In free space, the measured received power S21 on port 2 at the center frequency of 5.3 GHz is -39.88 dB. It is close to the estimated value of -38.97 dB. Figure 7(a) shows that the fiberglass EW-185 specimen exhibits relatively lower attenuation than the fiber carbon C522 Twill. The value of insertion-loss (S21) for the fiberglass EW-185 specimen is also very close to the insertion-loss (S21) value in free space. At the center frequency of 5.3 GHz, the measured attenuation of the fiberglass EW-185 specimen is -0.25 dB. The fiber carbon C522 twill contributes significantly to the attenuation with a measuring of -27.66 dB. These values indicate that the fiber E-glass EW-185 contributes -0.50 dB and the carbon C522 contributes -55.32 dB of attenuation for the CP-SAR signal strength in a round-trip propagation. Generally, this behavior is consistent with the circular depolarization data presented in Figure 7(b). The circular depolarization of the fiberglass EW-185 specimen is measured at 0.32 dB, while the fiber carbon C522 Twill significantly contributes 10.70 dB. The more detailed measurement value of the material attenuation and circular depolarization in the several frequencies of the bandwidth is listed in Table 3.

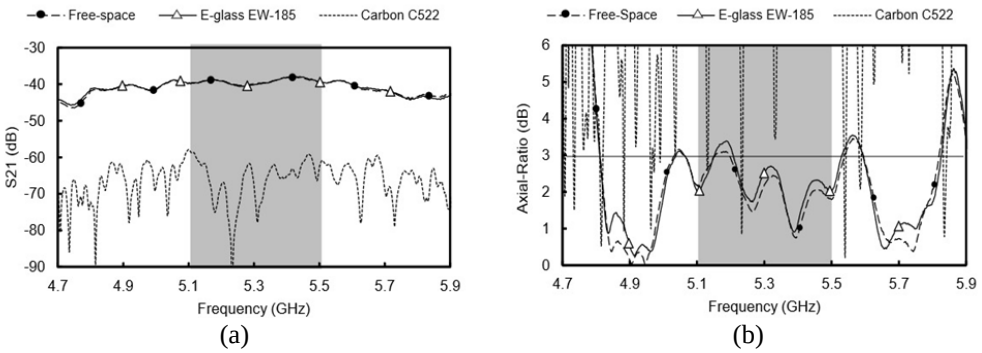

Figure 7. Measured characteristics of the CP-SAR antenna in spreading frequency; (a) received power in port 2 (S_{21}) and (b) AR

Table 3. Summarized material attenuation and circular depolarization of the CP-SAR antenna inside the composite materials of the LSU, measurement sampling on several frequencies of the bandwidth

Frequency f (GHz)	Received power S_{21} (dB)	Material attenuation (dB)		Axial- ratio AR (dB)	Circular depolarization (dB)	
		E –glass EW-185	Carbon C522		E-glass EW-185	Carbon C522
5.10	-39.81	0.15	-18.06	2.19	-0.17	69.33
5.15	-39.08	0.05	-22.61	2.96	0.00	14.52
5.20	-39.02	-0.10	-28.51	2.92	0.30	12.09
5.25	-40.25	-0.24	-34.69	1.67	0.18	8.94
5.30	-39.88	-0.25	-27.66	2.19	0.32	10.70
5.35	-39.33	-0.12	-23.98	2.09	0.07	16.51
5.40	-38.20	-0.05	-26.83	0.84	0.32	13.59
5.45	-38.23	-0.22	-23.02	2.04	0.28	29.84
5.50	-39.44	-0.12	-23.29	1.79	0.24	22.10

The experimental investigation of the radiation pattern characteristics of the CP-SAR antenna, when installed inside the LSU specimen material at frequencies of 5.1 GHz, 5.3 GHz, and 5.5 GHz, is plotted in Figure 8 (namely Figures 8(a)-(c), respectively). The radiation pattern was performed in the H-plane (ϕaz) and was deemed sufficient. Based on the graph, the effect of the composite specimen composed of the fiberglass EW-185 does not significantly alter the radiation pattern and 3-dB beamwidth of the CP-SAR antenna. The 3-dB beamwidth of the CP-SAR antenna in free space medium was measured at 21° and 23.0° inside the fiberglass specimen box- closely matching the CP-SAR antenna's specified 3-dB beamwidth of 22.0°. This result indicates that the fiberglass EW-185 with a thickness of 1.2 mm is suitable for manufacturing the LSU airframe.

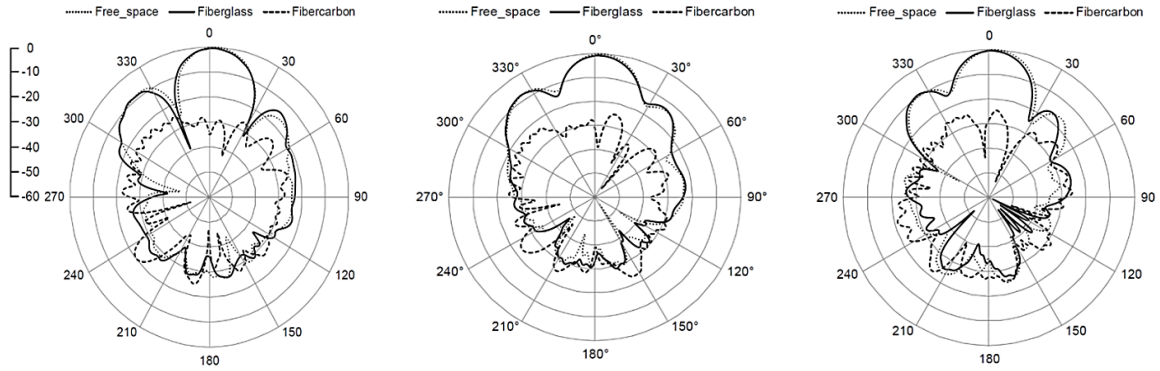

(a) (b) (c)

Figure 8. The radiation pattern of the CP-SAR sensor measured in a H-plane position at several frequencies; (a) 5.1 GHz, (b) 5.3 GHz, and (c) 5.5 GHz

In contrast, the measurement of the fiber Carbon C522 Twill reveals significant attenuation, and the main lobe of the CP-SAR antenna is no longer discernible. The 3-dB beamwidth of the CP-SAR antenna under these conditions becomes unacceptable. Further, the measured azimuth 3-dB beamwidth of the CP-SAR antenna inside the LSU at several frequencies in the H-plane (ϕaz) is summarized in Table 4.

Table 4. Summary of the measured azimuth 3-dB beam-width of the CP-SAR antenna inside the LSU at several frequencies in H-plane (ϕaz)

Frequency (GHz)	Azimuth 3-dB beam-width (ϕ_{az})		
	Free space	Fiber E-glass EW-185	Fiber carbon C522 twill
5.1	22.0°	24.0°	N/A
5.3	21.0°	23.0°	N/A
5.5	23.0°	23.0°	N/A

5. CONCLUSION

The experimental investigation on the effect of airframe materials of the LSU on the electromagnetic characteristics of the airborne CP-SAR antenna has been demonstrated and presented. The measurement result of the fiber E-glass EW-185 composite with 1.2 mm thickness at the frequency of

5.3 GHz shows the attenuation and circular depolarization reached approximately -0.25 dB and 0.32 dB, respectively. These values indicate the fiber E-glass EW-185 contributes -0.50 dB of attenuation to the CP-SAR signal strength for round-trip propagation and has no significant effect on the circular polarization performance. The fiber E-glass EW-185 composite with 1.2 mm thickness is still acceptable for an airframe material on a CP-SAR platform. On the other hand, the fiber Carbon C522 Twill composite has attenuation and circular depolarization of approximately -27.66 dB and 10.70 dB, respectively. These values show the fiber Carbon C522 Twill composite gives a high attenuation on both magnitude power and AR value. This observation suggests that the Carbon C522 Twill composite with a thickness of 1.1 mm is unsuitable for manufacturing an airborne remote sensing platform, specifically for accommodating the CP-SAR antenna. Despite its acknowledged benefits in lightweight properties and strong physical construction, this material does not meet the necessary criteria for this application. For future works, the research can improve with some suggestions like material variations, frequency range, and antenna position on the fuselage.

ACKNOWLEDGMENTS

This work is supported by the Riset-Pro Program of the Ministry of Research Technology and Higher Education of Indonesia (Ristekdikti), the Research Center for Aeronautics Technology, the National Research and Innovation Agency (BRIN), and the Center for Environmental and Remote Sensing (CEReS) Chiba University Japan.

FUNDING INFORMATION

This work is supported by the Riset-Pro Program of the Ministry of Research Technology and Higher Education of Indonesia (Ristekdikti) with World Bank Project Loan Number: 8245-ID.

AUTHOR CONTRIBUTIONS STATEMENT

This journal uses the Contributor Roles Taxonomy (CRediT) to recognize individual author contributions, reduce authorship disputes, and facilitate collaboration.

Name of Author	C	M	So	Va	Fo	I	R	D	O	E	Vi	Su	P	Fu
Wahyudi	✓	✓	✓		✓	✓	✓		✓	✓	✓		✓	
Imas Tri Setyadewi	✓	✓		✓		✓	✓	✓		✓	✓			✓
Mohammad Amanta Kumala Sakti		✓			✓	✓				✓	✓			
Yanuar Prabowo	✓	✓				✓		✓		✓				
Donatina Miswati Hadiyanti		✓				✓				✓			✓	
Novelita Rahayu		✓				✓				✓				
Nurul Lailatul Muzayadah	✓	✓	✓	✓	✓	✓	✓	✓	✓	✓				✓
Agus Hendra Wahyudi		✓		✓		✓	✓			✓			✓	✓
Yomi Guno		✓				✓				✓	✓			
Teguh Praludi		✓				✓				✓	✓			
Cahya Edi Santosa	✓	✓	✓	✓		✓	✓	✓	✓	✓		✓		
Josaphat Tetuko Sri Sumantyo		✓			✓	✓	✓			✓		✓		

C : **C**onceptualization
M : **M**ethodology
So : **So**ftware
Va : **Va**lidation
Fo : **Fo**rmal analysis
I : **I**nvestigation
R : **R**esources
D : **D**ata Curation
O : Writing - **O**riginal Draft
E : Writing - Review & **E**diting
Vi : **Vi**sualization
Su : **Su**pervision
P : **P**roject administration
Fu : **Fu**nding acquisition

CONFLICT OF INTEREST STATEMENT

Authors state no conflict of interest.

DATA AVAILABILITY

The data that support the findings of this study are available from the corresponding author, [initials: W], upon reasonable request.

REFERENCES

[1] D. H. Ai, V. L. Nguyen, H. H. Duc, and K. T. Luong, "On the performance of reconfigurable intelligent surface-assisted UAV-to-ground communication systems," *TELKOMNIKA (Telecommunication Computing Electronics and Control)*, vol. 21, no. 4, pp. 736–741, 2023, doi: 10.12928/TELKOMNIKA.v21i4.24720.

[2] M. Edrich and G. Weiss, "Second-generation Ka-band UAV SAR system," *Proceedings of the 38th European Microwave Conference, EuMC 2008*, pp. 1636–1639, 2008, doi: 10.1109/EUMC.2008.4751786.

[3] J. T. S. Sumantyo *et al.*, "Airborne Circularly Polarized Synthetic Aperture Radar," *IEEE Journal of Selected Topics in Applied Earth Observations and Remote Sensing*, vol. 14, pp. 1676–1692, 2021, doi: 10.1109/JSTARS.2020.3045032.

[4] R. Baqué, S. Angelliaume, P. D. Femandez, and O. R. du Plessis, "Ground penetrating capabilities of Airborne SAR System SETHI," in *2021 18th European Radar Conference (EuRAD)*, 2022, pp. 9–12, doi: 10.23919/EuRAD50154.2022.9784476.

[5] H. Huang *et al.*, "A Novel Method for Staggered SAR Imaging in an Elevation Multichannel System," *IEEE Transactions on Geoscience and Remote Sensing*, vol. 61, pp. 1–19, 2023, doi: 10.1109/TGRS.2023.3236988.

[6] J. C. Curlander and R. N. McDonough, "Synthetic Aperture Radar - Systems and Signal Processing-Wiley-Interscience (1991) | PDF | Microwave | Remote Sensing," 1991.

[7] M. Ding *et al.*, "A W-Band Active Phased Array Miniaturized Scan-SAR with High Resolution on Multi-Rotor UAVs," *Remote Sensing*, vol. 14, no. 22, 2022, doi: 10.3390/rs14225840.

[8] D. Wang, Y. Zhang, C. Yang, and K. Wang, "Study on processing synthetic aperture radar data based on an optical 4f system for fast imaging," *Optics Express*, vol. 30, no. 25, p. 44408, Dec. 2022, doi: 10.1364/oe.471716.

[9] J. Svedin, A. Bernland, and A. Gustafsson, "Small UAV-based high resolution SAR using low-cost radar, GNSS/RTK and IMU sensors," in *EuRAD 2020 - 2020 17th European Radar Conference*, 2021, pp. 186–189, doi: 10.1109/EuRAD48048.2021.00055.

[10] W. L. Stutzman, "Polarization in Electromagnetic Systems," *Journal of Chemical Information and Modeling*, vol. 53, no. 9, pp. 1689–1699, 2018.

[11] S. Dey, A. Bhattacharya, A. C. Frery, C. Lopez-Martinez, and Y. S. Rao, "A Model-Free Four Component Scattering Power Decomposition for Polarimetric SAR Data," *IEEE Journal of Selected Topics in Applied Earth Observations and Remote Sensing*, vol. 14, pp. 3887–3902, 2021, doi: 10.1109/JSTARS.2021.3069299.

[12] S. Gao, "Introduction to Circularly Polarized Antennas," in *Circularly Polarized Antennas*, Wiley, 2014, pp. 1–28, doi: 10.1002/9781118790526.ch1.

[13] S. Singh, H. G. Hanumantharaju, S. R. T. Yadla, S. H. R. Yadav, and S. Srivatsa, "Investigation of bending properties of E-Glass fiber reinforced polymer matrix composites for applications in micro wind turbine blades," *Journal of Physics: Conference Series*, vol. 1473, no. 1, p. 012047, Feb. 2020, doi: 10.1088/1742-6596/1473/1/012047.

[14] N. L. Muzayadah *et al.*, "Performance Analysis of Carbon Composite Materials with VARI Method for Electromagnetic Interference Applications," in *Proceeding - 2021 International Conference on Radar, Antenna, Microwave, Electronics, and Telecommunications: Managing the Impact of Covid-19 Pandemic: Together Facing Challenges Through Electronics and ICTs, ICRAMET 2021*, Nov. 2021, pp. 191–195, doi: 10.1109/ICRAMET53537.2021.9650351.

[15] R. Vangala, M. Devaiah, N. Rajendar, and K. Raju, "Comparison Of Mechanical Properties For Carbon, E-Glass And Hybrid (Carbon & E-Glass) Composites" *International Journal of Mechanical Engineering and Technology (IJMET)*, vol. 10, no. 2, pp. 407-417, Feb. 2019.

[16] C. Andrews, L. Boskovic, and D. S. Filipovic, "Characterization of Flat Radomes for (18 to 45) GHz High-Power Horn Antennas," *IEEE Transactions on Antennas and Propagation*, vol. 70, no. 3, pp. 2381–2386, 2022, doi: 10.1109/TAP.2021.3111664.

[17] X. Liu, Y. Zhou, C. Wang, L. Gan, X. Yang, and L. Sun, "Dual-Band Dual-Rotational-Direction Angular Stable Linear-to-Circular Polarization Converter," *IEEE Transactions on Antennas and Propagation*, vol. 70, no. 7, pp. 6054–6059, 2022, doi: 10.1109/TAP.2021.3138533.

[18] J. T. S. Sumantyo *et al.*, "Hinotori-C2 Mission : CN235MPA Aircraft Onboard Circularly Polarized Synthetic Aperture Radar (CP-SAR)," *International Geoscience and Remote Sensing Symposium (IGARSS)*, pp. 8538–8541, 2019, doi: 10.1109/IGARSS.2019.8899244.

[19] C. E. Santosa, J. T. S. Sumantyo, K. Urata, C. M. Yam, K. Ito, and S. Gao, "Development of a low profile wide-bandwidth circularly polarized microstrip antenna for C-band airborne CP-SAR sensor," *Progress In Electromagnetics Research C*, vol. 81, pp. 77–88, 2018, doi: 10.2528/pierc17110901.

[20] I. T. Setyadewi, Y. Prabowo, P. Wibowo, and P. S. Priambodo, "Unconsidered but influencing interference in unmanned aerial vehicle cabling system," *International Journal of Electrical and Computer Engineering (IJECE)*, vol. 14, no. 1, pp. 22–30, 2024, doi: 10.11591/ijece.v14i1.pp22-30.

[21] Sunar, A. S. Budiyanta, P. E. Broto, and A. B. Utama, "Analyze Angle of the Camera Payload LSU-02 in Mission of Aerial Photo," *International Symposium on Global Navigation Satellite System 2018 (ISGNSS 2018)*, vol. 94, 2019, doi: 10.1051/e3sconf/20199401015.

[22] J. Zouhar *et al.*, "Application of Carbon–Flax Hybrid Composite in High Performance Electric Personal Watercraft," *Polymers*, vol. 14, no. 9, p. 1765, Apr. 2022, doi: 10.3390/polym14091765.

[23] J. Li *et al.*, "Fabrication of Large Aerogel-Like Carbon/Carbon Composites with Excellent Load-Bearing Capacity and Thermal-Insulating Performance at 1800 °c," *ACS Nano*, vol. 16, no. 4, pp. 6565–6577, 2022, doi: 10.1021/acsnano.2c00943.

[24] G. V. Săftoiu, C. Constantin, A. I. Nicoară, G. Pelin, D. Ficai, and A. Ficai, "Glass Fibre-Reinforced Composite Materials Used in the Aeronautical Transport Sector: A Critical Circular Economy Point of View," *MDPI Sustainability*, vol. 16, no. 11, pp. 1-23, 2024, doi: 10.3390/su16114632.

[25] "3102 Conical Log Spiral Antenna," [Online]. Available: https://www.ets-lindgren.com/datasheet/antennas/conical-log-spiral/4011/401102.

[26] C. A. Balanis, *Antenna Theory Analysis and Design Third Edition*, John Wiley & Sons, 2016.

[27] J. Núñez, P. Orgeira-Crespo, C. Ulloa, and I. García-Tuñón, "Analysis of the operating conditions for UAV-based on-board antenna radiation pattern measurement systems," *PLoS One*, vol. 16, no. 2, pp. 1–21, 2021, doi: 10.1371/journal.pone.0245004.

BIOGRAPHIES OF AUTHORS

Wahyudi was born in Jakarta on December 28th, 1974. He completed his bachelor degree in Computer System from STMIK Budi Luhur in 2003 and obtained his master degree from University Indonesia in 2010. Currently he is a work as researcher in Research Centre of Aeronautics–National Research and Innovation Agency–Indonesia. His area of interest is computation and network technology. He is also interest in datalink for aerial vehicle for control and data transmission. He can be contacted at email: wahy023@brin.go.id.

Imas Tri Setyadewi received a B.Sc. degree in Physics Faculty of Mathematics and Science, in 2012 and a Master's degree in Electrical Engineering with a major in Electronics and Smart Embedded Systems in 2022 from Universitas Indonesia (UI). She has been working in the Government sector at the National Research and Innovation Agency (BRIN) as UAV Engineer since 2014. Her research interest includes electromagnetic field, electrical system, and avionics. She can be contacted at email: imas003@brin.go.id.

Mohammad Amanta Kumala Sakti was born in Jakarta on November 23rd, 1983. He received his bachelor's degree in Telecommunication Engineering from Universitas Trisakti Jakarta in 2007 and obtained his master's degree in Telecommunication Engineering from Universitas Indonesia in 2017. Since 2010 until now, he has been working at Agency for the Assessment and Application of Technology, which has now changed to the National Research and Innovation Agency (BRIN). His research interest is focused on antenna technology and radio frequency. He can be contacted at email: moha039@brin.go.id.

Yanuar Prabowo was born in Surabaya, Indonesia. He obtained a Bachelor's degree in electrical engineering in 2008 from Institut Teknologi Sepuluh Nopember (ITS), Surabaya, Indonesia, and a Master's degree in Electrical Engineering with a major in Telecommunication Engineering in 2017 from Universitas Indonesia in Depok, Indonesia. He has worked as a researcher at National Research and Innovation Agency, at the Aeronautics and Space Research Organization at BRIN since 2010. His research interest includes datalink communications, avionic, antennas, and RF components. He can be contacted at email: yanu004@brin.go.id.

Donatina Miswati Hadiyanti was born in Yogyakarta on September 6th 1964. She completed a bachelor's degree in mathematics from Gadjah Mada University in 1989. She is currently a Research Staff with the Aviation Technology Research Center of The National Research and Innovation Agency (BRIN). Her research areas being developed are data link communication systems and aviation navigation. She can be contacted at email: dona001@brin.go.id.

Novelita Rahayu is a Researcher at the Badan Riset dan Inovasi Nasional (BRIN), Indonesia. She received her Master Degree in Electrical Engineering from Institut Teknologi Bandung, Indonesia, and currently, she is pursuing her doctoral candidate in Electrical Engineering and Informatics at Institut Teknologi Bandung, Indonesia. Her research interests primarily revolve around active and passive radio frequency systems, antennas, and electromagnetic compatibility/interference (EMC/I). She has published numerous publications in IEEE. Her work has brought her to meet another researchers and academics for research collaborations. She can be contacted at email at: novelitarahayu@ieee.org or nove001@brin.go.id.

Nurul Lailatul Muzayadah was born in Jember on August 23, 1995. She received her bachelor degree in Materials Engineering Institute Teknologi Sepuluh Nopember in 2017. Currently, she is doing her master's degree at Central South University, majoring in Materials and Chemicals. Her research interests include composites, electromagnetics, and processing materials. She can be contacted at email: nuru031@brin.go.id

Agus Hendra Wahyudi received a Bachelor's degree in Engineering in Electrical Engineering from Brawijaya University, Indonesia, in 2003, and a Master's degree in Instrumentation Physics from University of Indonesia, in 2010. Received his Ph.D. in Information Science from Chiba University, Japan in 2019. He is currently a young researcher at Research Center for Aeronautics Technology, National Research and Innovation Agency (BRIN), and a lecturer in the Department of Electrical Engineering at Universitas Pamulang Indonesia. His current research interests include antennas, instrumentation, SAR sensors, and telecommunications. He can be contacted at email: agus111@brin.go.id and agus8hendra@gmail.com.

Yomi Guno received his Bachelor of Science in Physics from Padjadjaran University, Indonesia, in 2003 and subsequently obtained a Master's degree in Telecommunications Engineering from Universitas Indonesia in 2015. He is currently pursuing a Ph.D. in Electronics and Informatics at Bandung Institute of Technology, Bandung, Indonesia, under the supervision of Prof. Trio Adiono. Presently, he serves as a middle expert researcher at the National Research and Innovation Agency of the Republic of Indonesia. His research interests are signal processing, unmanned aerial vehicles (UAVs), telecommunications, orthogonal frequency-division multiplexing (OFDM), and UAV communication channels. He can be contacted at email: yomi.guno@brin.go.id.

Teguh Praludi received the B.S. degree in electrical engineering from Diponegoro University, Semarang, Indonesia in 2003 and the M.Eng. degree from the Bandung Institute of Technology, Bandung, Indonesia, in 2013. Since 2003, he has been a Researcher with Center for Telecommunication and electronic at Indonesian Institute of Sciences, and then in 2019 reseacher in center Telecommunication National Research and Innovation Agency (BRIN), Bandung, Indonesia. His research interests include the development of filter for telecommunication, and moduls of radar and microwave. He can be contacted at email: tegu012@brin.go.id.

Cahya Edi Santosa (Member, IEEE) received the B.Eng. degree in electrical engineering from Gadjah Mada University, Yogyakarta, Indonesia, in 2003 and the M.Eng. degree from the Bandung Institute of Technology, Bandung, Indonesia, in 2013. Since 2003, he has been a Researcher with Center for Aeronautics Technology, National Institute of Aeronautics and Space (LAPAN), Jakarta, Indonesia. Since 2021, he has been a Senior Researcher with Center for Aeronautics Technology, National Research and Innovation Agency (BRIN), Jakarta, Indonesia. His research interests include the development of antennas for telecommunication, unmanned aerial vehicle, and synthetic aperture radar. He can be contacted at email: cahy012@brin.go.id.

Dr. Josaphat Tetuko Sri Sumantyo (Senior Member, IEEE) was born in Bandung, Indonesia, in 1970. He received the B.Eng. and M.Eng. degrees in electrical and computer engineering (subsurface radar systems) from Kanazawa University, Kanazawa, Japan, in 1995 and 1997, respectively, and the Ph.D. degree in artificial system sciences (applied radio wave and radar systems) from Chiba University, Chiba, Japan, in 2002. From 2002 to 2005, he was a Lecturer (Postdoctoral Fellowship Researcher) with Center for Frontier Electronics and Photonics, Venture Business Laboratory, Chiba University. From 2005 to 2013, he was an Associate Professor (permanent staff) with the Center for Environmental Remote Sensing, Chiba University, where he is currently a Full Professor (permanent staff). Since 2019, he has been the Head of the Department of Environmental Remote Sensing and Head Division of Earth and Environmental Sciences, Graduate School of Integrated Science and Technology, Chiba University. He has authored or coauthored about 700 journal and conference papers, and tens of books related to wave analysis, SAR, and small antennas. His research interests includes theoretically scattering microwave analysis and its applications in the microwave (radar) remote sensing, especially synthetic aperture radar and subsurface radar (VLF), including InSAR, DInSAR, and PS-InSAR, analysis and design of antennas for mobile satellite communications and microwave sensors, development of microwave sensors, including synthetic aperture radar (SAR) for the unmanned aerial vehicle, aircraft, and microsatellite. He is the General Chair of the 7th Asia-Pacific Conference on Synthetic Aperture Radar (APSAR 2021) at Bali, Indonesia, and more than 200 invited talks and lectures related to synthetic aperture radar and its applications. He is the Co-Leader of the Working Group on remote sensing instrumentation and technologies for unmanned aerial vehicles of IEEE Geoscience and Remote Sensing Society and Technical Committee on Instrumentation and Future Technologies. He can be contacted at email: jtetukoss@faculty.chiba-u.jp and jtetukoss@nifty.com.